Asian Journal of Physics Vol. 15, No. 1 (2006) 1-14

In vivo investigation of human skin optical clearing and blood microcirculation under the action of glucose solution

Alexey N Bashkatov[1], Alexander N Korolevich[2,3], Valery V Tuchin[1], Yuri P Sinichkin[1], Elina A Genina[1], Mikhail M. Stolnitz[1], Nataly S Dubina[4], Sergey I Vecherinski[4], Michael S Belsley[2]

[1] *Institute of Optics and Biophotonics, Department of Optics and Biomedical Physics of Saratov State University, Saratov, Russia*

[2] *Physical Department, Minho University, Campus Gualtar, 4709 Braga, Portugal*

[3] *B I Stepanov Institute of Physics of National Academy of Sciences of Belarus, Skarina Ave., 68, 220072 Minsk, Belarus*

[4] *GP "MTZ Medservice", 220009 Minsk, Belarus*

We present experimental results on optical properties of the human skin controlled by administration of the 40%-glucose solution. *In vivo* reflectance spectra of the human skin were measured. Results of the experimental study of influence of the 40%-glucose solution on reflectance spectra of the human skin are presented. A significant decrease of reflectance of the human skin under action of the osmotic agent is demonstrated. The experiments show that administration of the glucose solution allows for effective control of tissue optical characteristics, that makes skin more transparent, thereby increasing the ability of light penetration through the tissue. Laser Doppler flowmetry has been used for study of skin blood microcirculation under the action of the glucose solution. Results of the experiments demonstrated that at the action of the glucose solution blood perfusion and blood concentration increase, however the mean blood velocity does not change. The presented results can be used in developing functional imaging techniques, including OCT and reflectance spectroscopy. A potential benefit of the optical clearing technique is the improvement of laser therapeutic techniques that rely on sufficient light penetration to a target embedded in tissue.

1 Introduction

Recent technological advancements in the photonics industry have led to a resurgence of interest in optical imaging technologies and real progress toward the development of non-invasive clinical functional imaging systems. Over the last decade, non-invasive or minimally invasive spectroscopy and imaging techniques have witnessed widespread exciting applications in biomedical diagnostics, for example, optical coherence tomography (OCT) [1,2], visible and near-infrared elastic-scattering spectroscopy [3,4], fluorescent [1,3,5] and polarisation spectroscopy [6,7]. Spectroscopic techniques are capable of deep-imaging of tissues that could provide information of blood oxygenation [8] and detect cutaneous, brain and breast tumours [9], whereas confocal microscopy [10], OCT [2,11-13], and multi-photon excitation imaging [10,14] have been used to show cellular and sub-cellular details of superficial living tissues. Spectroscopic and OCT techniques are applicable for blood glucose monitoring with diabetic patients [15-17]. Besides diagnostic applications optical methods are widely used in modern medicine, for example, for photodynamic therapy [18-20], and for laser surgery of different diseases [21,22]. Interest in using optical methods for physiological-condition monitoring and cancer diagnostics and therapies has been increased due to their simplicity, safety, low cost, contrast and resolution features in contrast to conventional X-ray computed tomography and ultrasound imaging [9].

The main limitations of the majority of the imaging techniques, including OCT and near-infrared (NIR) spectroscopy deal with the strong light scattering in superficial tissues [9,23-26], which cause decrease of spatial resolution, low contrast, and small penetration depth. Solution of the problem, i.e. reducing of light scattering, and thus improving of image quality and precision of spectroscopic information, can be connected with control of tissue optical properties.

The optical properties of biological tissues can be effectively controlled by compression [27], dehydration and coagulation [28], staining [29,30], and others actions. Such control means the change of the scattering or absorption properties of a tissue.

It is well-known that the major source of scattering in tissues and cell structures is the refractive index mismatch between cell organelles, like mitochondria, and cytoplasm, extracellular media and tissue structural components such as collagen and elastin fibres [9,12,31-35]. The tissue scattering properties can be significantly changed due to action of osmotically active immersion liquids [9,26,31,32,36-57]. Similar results have been obtained for optical clearing of whole blood [25,58-60]. Administration of the immersion liquid having a refractive index higher than that of tissue interstitial fluid induces a partial replacement of the interstitial fluids by immersion substance and hence, matching of refractive indices of tissue scatterers and the interstitial fluid. Osmotic activity of the immersion agents may cause tissue dehydration, that also equalizes refractive indices within tissue. The matching, correspondingly, causes the decrease of scattering. As osmotic immersion liquids aqueous solutions of glucose and mannitol, propylene glycol, glycerol and other biocompatible chemicals are used.

Glucose solutions are widely used for the control of tissue scattering properties in consequence of biocompatibility of glucose. The aqueous glucose solutions were used for optical clearing of skin [37,41,43,47,53,55], sclera [36,38,39,44], dura mater [45,57], etc.

The possibility of selective translucence of the superficial skin layers is very useful in developing functional imaging techniques, including OCT and reflectance spectroscopy. A potential benefit of the optical clearing technique is the improvement of laser therapeutic techniques that rely on sufficient light penetration to a target embedded in tissue. Combining optical clearing with laser radiation could reduce the laser fluences required for a therapeutic effect. Another application of the optical method is the non-invasive visualisation of cutaneous blood microvessels and small pathologic structures in tissues (including cancerous growth) with a high resolution. This is important for diagnosis and treatment of many diseases such as tumours of skin, vascular pathologies, diabetes, etc. A specific application that may benefit from the optical clearing technique is blood photocoagulation [48]. The result shows that significantly lower laser irradiances could be required to irreversible damage of targeted blood vessels in skin treated with a hyperosmotic agent and thus the damage of collateral tissue can be minimised. However, despite the numerous studies, the exact mechanism of the skin optical clearing is still unclear due to complex morphological nature of skin with many inhomogeneities.

Previous *in vivo* investigations of skin optical clearing [37,40,41,43,46-48,55] showed that the method of delivery of clearing agent into skin is very important. Intradermal injection of glucose or glycerol solutions is preferably in comparison with topical application of the agents due to protective properties of upper layer of skin, the stratum corneum. The layer is composed of corneocytes embedded in hydrophobic lipid domains [61,62]. The majority of these lipids form crystalline lamelar phases. The corneocytes are filled with cross-linked soft keratin [63]. One of the main destinations of stratum corneum is barrier function of skin, i.e. regulation of transepidermal water loss and preventing penetration some substances from environment into the body. In this way penetration of clearing agents in skin are difficult and need special techniques for enhancement of the stratum corneum permeability. Iontophoresis is a widely used method that is applied in clinical practice for transcutaneous drug delivery [64], but the method is complicated and may be used for polar substances only.

For investigation of the optical clearing the various spectroscopic techniques have been used (for example the technique of integrating spheres measurements [36,39,40,43,46,51,56,57], measurements of collimated transmittance [36,38-45], OCT [25,26,47,48,52,53] etc), but only reflectance spectroscopy [37,38,40,41,43,47,55] and OCT can be used in case of *in vivo* measurements.

Since in case of intradermal injection of clearing agent (such as glucose solution) blood is a primary carrier of the agent, the investigation of skin blood microcirculation at administration of clearing agents in skin is very important for clarification of mechanisms of the tissue clearing *in vivo*. Laser Doppler flowmetry is a technique that has found an increasing utility in the skin research [48,65]. It measures cutaneous perfusion by scanning a low-power laser beam over a region of skin. When monochromatic light interacts with a moving object such as a blood cell, a slight change in frequency of the scattered light induced due to the Doppler effect, whereas the light backscattering from non-moving tissue structures

remains at the same frequency. The frequency shift is dependent on the average speed of the blood cells, while the magnitude of the returning Doppler signal relates to the number of moving cells. At each measurement site, the backscattered laser light is detected by a photodetector contained in the scanning head of the instrument and the resulting signal is used to calculate the degree of tissue perfusion, which is expressed in arbitrary units.

In this study, we investigate skin optical clearing and the skin blood microcirculation *in vivo* under the action of 40% glucose solution.

2 Skin structure

Skin presents a complex heterogeneous tissue where blood and pigment content are spatially distributed variably in depth [66-68]. Skin consists of three main layers from the surface: epidermis (100 μm thick, the blood-free layer), dermis (1-2 mm thick, vascularised layer), and subcutaneous fat (from 1 to 6 mm thick, in dependence of the body site). Typically, the optical properties of the layers are characterised by the absorption μ_a and the scattering μ_s coefficients, which are equal to the average number of absorption and scattering events per unit path length of photon travel in the tissue and the anisotropy factor *g*, which represents the average cosine of the scattering angles.

The randomly inhomogeneous distribution of blood and various chromophores and pigments in skin produces variations of average optical properties of skin layers. Nonetheless, it is possible to define the areas in skin, where the gradient of skin cells structure, chromophores or blood amounts changing with a depth equals roughly zero [66]. This allows subdividing these layers into sublayers regarding the physiological nature, physical and optical properties of their cells, and pigment content. The epidermis can be subdivided into two sublayers: non-living and living epidermis. Non-living epidermis or stratum corneum (about 20 μm thick) consists of only dead squamous cells, which are highly keratinised with a high lipid and protein content, and has a relatively low water content [66,67]. Living epidermis (100 μm thick) contains most of the skin pigmentation, mainly melanin, which is produced in the melanocytes [69]. Large melanin particles such as melanosomes (> 300 nm in diameter) exhibit mainly forward scattering. Whereas, melanin dust, whose particles are small (< 30 nm in diameter), has the isotropy in the scattering profile, and optical properties of the melanin particles (30-300 nm in diameter) may be predicted by the Mie theory.

Dermis is a vascularised layer and the main absorbers in the visible spectral range are the blood haemoglobin, carotene and bilirubin. In the IR spectral range absorption properties of skin dermis are determined by absorption of water. Following the distribution of blood vessels [68] skin dermis can be subdivided into four layers: the papillary dermis (150 μm thick), the upper blood net plexus (100 μm thick), the reticular dermis (1-2 mm thick) and the deep blood net plexus (100 μm thick).

The scattering properties of the dermal layers are mainly defined by the fibrous structure of the tissue, where collagen fibrils are packed in collagen bundles and have lamellae structure. Light scatters on both single fibrils and scattering centres, which are formed by the interlacement of the collagen fibrils and bundles. To sum up, the average scattering properties of the skin are defined by the scattering properties of the reticular dermis because of relatively big thickness of the layer (up to 2 mm) and comparable scattering coefficients of the epidermis and the reticular dermis. Absorption of haemoglobin and water of skin dermis and lipids of skin epidermis defines the absorption properties of whole skin.

The subcutaneous adipose tissue is formed by aggregation of fat cells (adipocytes) containing stored fat (lipids) in a form of a number of small droplets for lean or normal humans and a few or even single big drop in each cell for obesity humans; and the lipids of mostly presented by triglyceride [70,71]. Content of the lipids in a single adipocyte is about 95% of its volume. The diameters of the adipocytes are in the range from 15 to 250 μm [72] and their mean diameter is varied from 50 [70] to 120 μm [71]. In the spaces between the cells there are blood capillaries (arterial and venous plexus), nerves and reticular fibrils connecting each cell and providing metabolic activity of fat tissue [70,71]. Absorption of the human adipose tissue is defined by absorption of haemoglobin, lipids and water. The main scatterers of adipose tissue are spherical droplets of lipids, which are uniformly distributed within adipocytes.

3 Materials and methods

3.1 Experimental setups

The *in vivo* spectroscopic experiments have been performed using multichannel optic spectrometer LESA-6med (BioSpec, Russia). The scheme of the *in vivo* experiments is shown in figure 1. As a light source, a 250 W xenon arc lamp with filtering of the radiation in the spectral range from 400 to 800 nm has been used in the measurements. Light was delivered to the skin and collected from the skin tissue using the originally designed optical probe, which consists of two optical fibres. Both fibres had 400 μm in core diameter and a numerical aperture of 0.2. The fibres have been enclosed in aluminium jacket (8-mm outer diameter) to provide a fixed distance between the fibres and the tissue surface. The central fibre has been placed in perpendicular to skin surface and delivers incident light to the skin surface. Distance between delivering fibre and skin surface is 12 mm. Diameter of the illuminated spot is about 5 mm. The collecting fibre is mounted at angle of 20° regarding to central fibre. Distance between tip of collecting fibre and skin surface is 20 mm and, in this geometry, light has been collected from area with diameter about 8 mm. The spectrometer was calibrated using a white slab $BaSO_4$ with a smooth surface.

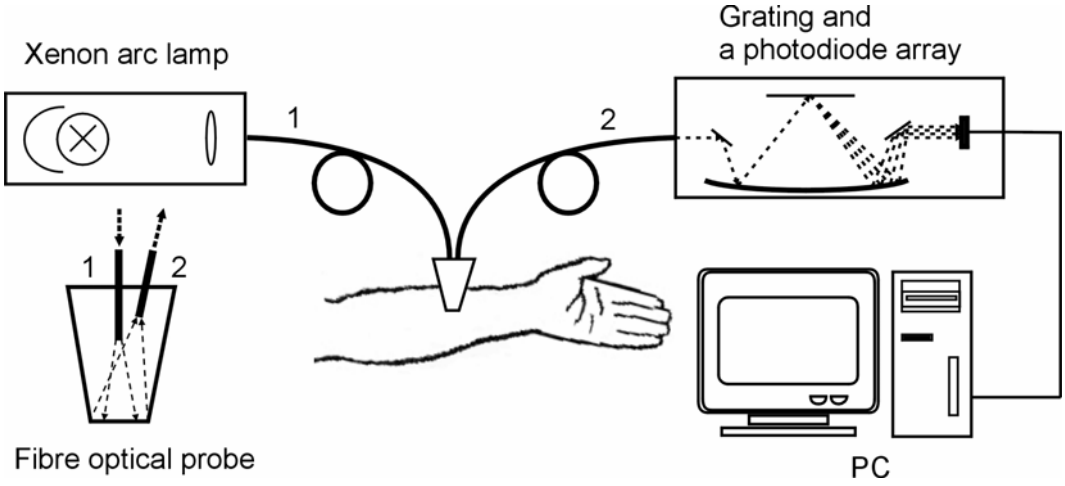

Fig. 1. Experimental set-up for measurements of the reflectance spectra:
1 – optical irradiating fibre; 2 – optical receiving fibre

The flowmetry and perfusion measurements were carried out using a commercially available PeriFlux 4001 setup from Perimed (Stockholm, Sweden). This instrument uses coherent laser radiation with the wavelength of 780 nm and the power of 0.8 mW. The radiation from the semiconductor diode laser passed through lens to be coupled into the light-guiding fibre with the aid of which it is guided to the surface of the object being investigated. Flexible fibre-optics laser probe was attached to the patient's body so that the laser radiation is incident perpendicularly to the skin's surface (see fig. 2).

The light is delivered to the probes via a flexible optical fibre with a very little loss of light. Flexible probe holders mould easily to the skin surface and are fixed with a double sided adhesive disc to hold the position of probes. The optical fibre is collecting the light back-scattered light from both static and moving components within the tissue.

In this study, we do not measure the absolute value of the blood velocity, only a change in the average value of the velocity. For the relative measurements, two detectors have been used. The first one was positioned on the left and the second on the right forearm of the healthy volunteer as a comparison channel. In this case the temporal intensity signal $I(t,x,y)$ obtained at each measurement location point (x,y) can be transformed into the frequency domain and results in the local power spectra $S(f,x,y)$.

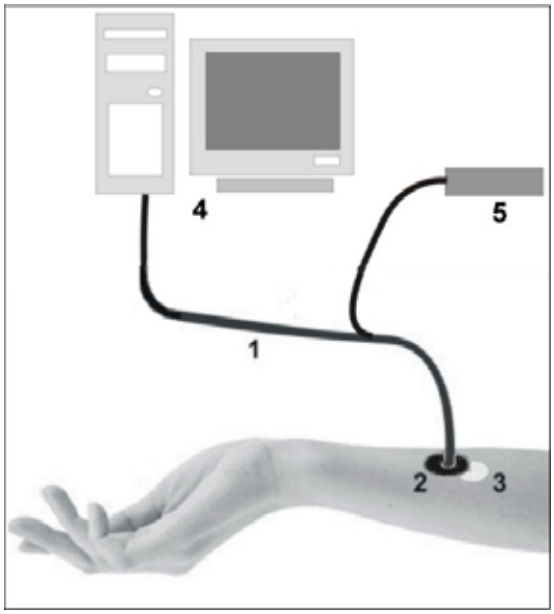

Fig. 2. Scheme of experimental setup for measurement of blood perfusion: 1 – optical cable which has two optical fibres; 2 – the double sided adhesive disc to hold the position of the optical cable; 3 – the place of glucose injection (the light circle is the swelling of the skin); 4 – computer; 5 – diode laser

The software of the PeriFlux 4001 uses the power spectrum to obtain the following three parameters.

- The integral of the power spectrum over all frequencies (resulting in a number proportional to the total number of moving red blood cells in the measurement volume), i.e. concentration of the particles:

$$Conc(x,y) = \int_a^b S(f,x,y)df \ . \tag{1}$$

- Microvascular perfusion (i.e. red blood cells flux) is defined as the first moment of the power spectrum:

$$Perf(x,y) = \int_a^b S(f,x,y)\, fdf \ . \tag{2}$$

- Mean velocity of the red blood cells is the value of the frequency shift, obtained as:

$$Vel\left(x,y\right)=\int_{a}^{b}S(f,x,y)\,fdf\;/\left(\int_{a}^{b}S(f,x,y)df+S(0,x,y)\right). \quad (3)$$

3.2 Experimental protocol

The measurements were carried out on the practically healthy volunteers of both sexes with ages from 24 to 60 years. Glucose solution was injected slowly into the dermal layer of skin (approximately 0.1 ml) of the volunteers forearm since the intradermal injection of the osmotically active agent is a more acceptable way to decrease scattering properties of skin. In this case, the protective properties of the stratum corneum barrier will be avoided. The measurement of dynamics of the optical clearing was started in 60 sec after the injection. All volunteers gave their informed consent for participation and the study protocol.

3.3 Immersion liquid

In this study, the commercially available 40%-aqueous glucose solution (DalChemPharm, Russia) has been used as a clearing agent. Composition of the solution is the following: dry glucose - 400 g, solution of hydrochloric acid with concentration 0.1M (up to pH of the prepared solution 3.0-4.0), sodium chloride - 0.26 g, distilled water up to one litre. The refractive index of the glucose solution has been measured by Abbe refractometer at wavelength 589 nm as 1.39 and pH of the solution have been measured by pH-meter "HANNA" (Portugal) as 3.5 using the standard method.

4 Results and Discussion

Figures 3 and 4 demonstrated optical clearing of human skin after administration of glucose solution into forearm of a volunteer. Fig. 3 shows reflectance spectra measured in the spectral range from 400 to 800 nm concurrently with administration of the 40%-glucose solution at different time intervals. From the figure it is seen that during one hour the skin reflectance decreases. It is connected with decreasing of the skin scattering properties due to the partial replacement of skin interstitial fluid by glucose solution.

In the spectral range 400-800 nm, the form of the presented spectra is defined by the absorption bands of blood of the upper and deep blood net plexus of skin with maxima at 420, 540 and 575 nm, and the spectral dependence of the scattering properties of the reticular dermis. Absorption of water in this spectral range is negligible [73]. The main scatterers of the dermal layer are collagen fibrils packed in collagen bundles and scattering centres, which are formed by the interlacement of the collagen fibrils and bundles. Fig. 3 shows, that during the optical clearing the dips in the spectra corresponding to blood absorption bands are decreased. This decreasing is connected with decreasing of skin scattering due to the matching effect, i.e. matching of refractive indices of the skin scatterers and interstitial fluid. The decrease of skin scattering produces change of regime of photon scattering from multiple to low, and the change leads to the increase of photon's free path length. Thus, more photons pass to subcutaneous adipose layer and the number of interactions of the photons with skin blood decreases. Hence, decrease of the absorbed fraction of light which leads to decreasing of the dips in the reflectance spectra is observed.

In the spectral range from 650 to 800 nm spectral signature of the reflectance spectra changes insignificantly. However, at initial moment reflectance decreases with wavelength increasing, but after 60 min of the optical clearing the reflectance increases with the wavelength increasing. That is connected with differences in the wavelength dependencies of the skin interstitial fluid at initial moment and after 60 min of the optical clearing since penetration of the glucose solution into skin produces a partial replacement of the interstitial fluids by the immersion substance. The time (60 min) corresponds to the minimal value of reflectance and thus maximal degree of optical clearing due to the magnitude of the

reflectance is manly determined by the tissue scattering and hence minimal value of the reflectance corresponds to minimal scattering and maximal value of glucose concentration in the skin interstitial fluid.

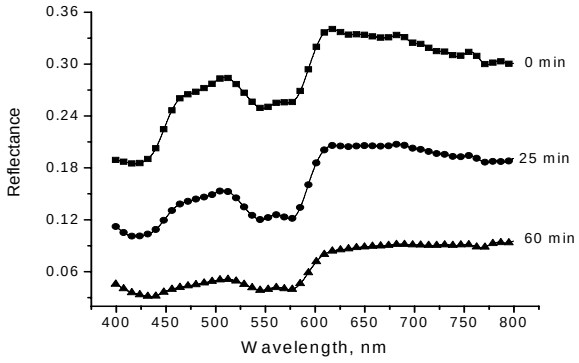

Fig. 3. The *in vivo* reflectance spectra of the human skin measured concurrently with administration of the 40%-glucose solution at different time intervals. The symbols correspond to the experimental data.

Fig. 4 presents dynamics of the reflectance measured at different wavelengths. From the figure it is very well seen that immediately after glucose injection the skin reflectance significantly decreases. During the first 20 min the reflectance increases but during the following time interval from 20 to 60 min skin reflectance decreases again. In the time interval from 60 to 140 min the skin reflectance increases slowly, with oscillating behaviour increasing.

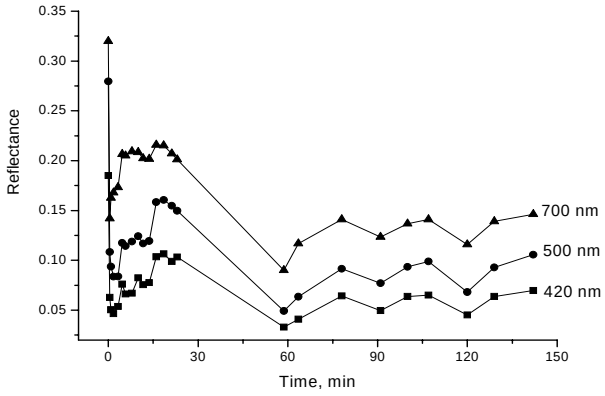

Fig. 4. The *in vivo* time-dependent reflectance of the human skin measured at different wavelengths concurrently with administration of the 40%-glucose solution. The symbols correspond to the experimental data.

The significant decreasing of reflectance, observed at initial moment, is connected with changing geometry of the experiment after glucose injection. The injected solution forms a vesicle filled with the glucose solution in skin, and the vesicle is observed on the skin surface as a swell. Presence of the swell

reduces the distance between the collecting fibre and skin surface, decrease of area of detection of backreflected radiation, and hence decrease of the reflectance.

Sizes of the vesicle have been measured by ultrasonography using 7.5 MHz diagnostic ultrasound system (Model SSH-140A, Toshiba, Japan) and standard method of measurements. In 1 min after injection the width of the vesicle is 5.4 mm, length is 6.3 mm, depth (i.e. distance between skin surface and the vesicle) is 1.5 mm. In 2 min after injection the width of the vesicle is 6 mm, length is 8.4 mm, depth is 1.5 mm. In 3 min after injection the width is 8.6 mm, length is 9.8 mm, depth is 1.2 mm. In 4 min after injection the width is 10.2 mm, length is 13.3 mm, and depth is 1.0 mm.

Injection of the 40%-glucose solution creates the virtual transparent window in skin and the window was observed during about 30 min. Such window allows one to clearly identify visually blood microvessels in the skin by the naked eye [55,74]. The swelling white ring appears around the window after the agent injection. The images of skin after intradermal injection of glucose were recorded by a digital video camera and diameters of the swelling area and the transparent window were measured [74]. The results presented in Fig. 5 (symbols). For the glucose injection, the diameter of the window was registered at the 1st min after injection. At the 2d min the diameter slightly decreases. For the next 15 min the diameter and diameter of the swelling area did not change. Since 20th min the significant reduction of the window was observed. Assuming that the shape of the vesicle can be presented as an ellipsoid of rotation and taking into account the temporal evolution of the diameter's of the swelling area the height of the swell can be calculated. In 1 min after injection the height is 3.5 mm. During first 5 min after injection the height of the swell decreases to 2.4 mm. In the next 10 min (from 5 to 15 min after glucose injection) height of the swell does not change. In 30 min after injection the swell on the skin surface disappears. The data can be very well approximated by the following polynomials (Eqs. 4-6) and the result of the approximations is presented in figure 5.

The temporal dynamics of the diameter of the virtual transparent window can be approximated by the polynomial approximation:

$$d = 4.839 - 0.939t + 0.209t^2 - 0.023t^3 + 1.32 \cdot 10^{-3} t^4 - 3.83 \cdot 10^{-5} t^5 + 4.31 \cdot 10^{-7} t^6, \quad (4)$$

where d is the diameter of the virtual transparent window, mm, and t is time, sec.

The temporal dynamics of the diameter of the swelling area can be approximated by the expression:

$$d = 7.66 - 1.9t + 0.5t^2 - 0.07t^3 + 5.7 \cdot 10^{-3} t^4 - 2.5 \cdot 10^{-4} t^5 + 5.9 \cdot 10^{-6} t^6 - 5.7 \cdot 10^{-8} t^7. \quad (5)$$

Here d is the diameter of the swelling area, mm.

The temporal dynamics of the height of the swell can be approximated by:

$$h = 4.043 - 0.518t + 0.055t^2 - 2.431 \cdot 10^{-3} t^3 + 3.391 \cdot 10^{-5} t^4, \quad (6)$$

where h is the height of the swell, mm.

In the figure it is seen, that the approximations describe very well the experimental data.

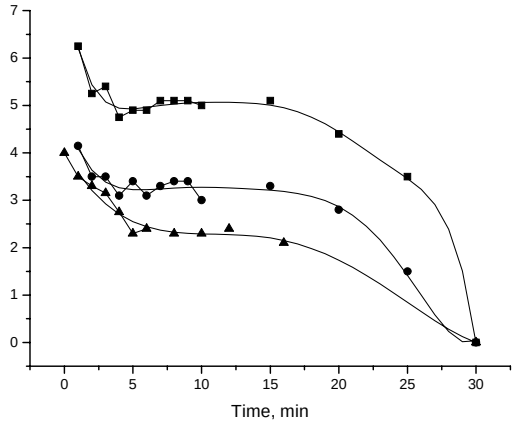

Fig. 5. The changes of skin reaction on injection of 40%-glucose solution. The symbols correspond to the experimental data: ● - the diameter of virtual transparent window, mm; ■ - the diameter of swelling area around the window, mm [55,74]; ▲ – the height of the swell, mm. The solid line correspond to the polynomial approximations (Eqs. 4-6)

Based on the temporal dynamics of the diameter of the swelling area (Eq. 5) and the temporal dependence of the height of the swell (Eq. 6) the temporal dynamics of the area of detection of backreflected radiation was calculated and the result is presented in Fig. 6. From the figure it is clearly seen that the temporal dependence is very well correlated with the temporal dynamics of skin reflectance presented in figure 4, and thus the temporal dependence of area of detection can be used for explanation of the temporal dynamics of skin reflectance at intradermal administration of the glucose solution.

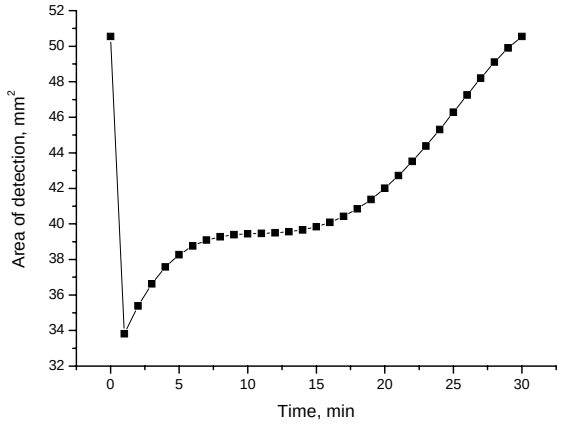

Fig. 6. The temporal dynamics of changes of the area of detection of backreflected radiation

We suppose, that, in general, the scheme of the optical clearing is the following. During glucose injection (within 5-10 sec) the clearing agent forms vesicle filled of the aqueous solution of glucose in skin dermis. Since skin dermis is elastic porous medium and the glucose solution is incompressible liquid then tissue surrounding of the vesicle is compressed and packs, its porosity is decreases [75] and

interstitial fluid is extruded from pores of the dermis. In the initial time interval from 0 to 5 min after injection the size of the vesicle decreases significantly under the influence of mechanical pressure of deformed skin tissues. In the time interval from 5 to 15 min the skin pressure is compensated by elastic properties of the glucose solution, and, as a result, the skin reflectance (and size of swell on the skin surface) does not change. The result can be explained within framework of the percolation theory [76], since it is necessary for glucose to form "infinite cluster" through surrounding layer of condensed tissue. Hence, the concentration of glucose solution in skin tissue surrounding the glucose vesicle is insignificant and the skin reflectance does not change (see fig. 4).

During time interval from 20 to about 60 min glucose solution diffuse from the vesicle to the surrounding of the vesicle skin tissue and corresponding tissue clearing takes place. The glucose-injected region became more transparent. Skin scattering decreases and, as consequence of this the reflectance of the skin decreases in about 3.8 times in an hour after clearing agent injection and then increases gradually, that shows the beginning of glucose diffusion from the observed area and corresponding reduction of tissue immersion. On the basis of the experiments, one can conclude that partial matching of refractive indices of the collagen fibres of dermis and the interstitial medium under action of 40%-glucose solution makes the main contribution to tissue clearing. It should be noted that skin has been transparent during a few hours. The second phase of tissue interaction with glucose is connected with taking down of the matching effect. It is determined by diffusion of glucose along the skin surface between two cellular layers a few orders less permeable – epidermal and subdermal fat cells. For the used aperture of the detector system, optical clearing was seen during a few hours.

It should be noted that the effect of tissue clearing was similar to that seen in the excised skin specimens [41,43]. Figures 7 and 8 show results of *in vitro* measurements of temporal dynamics of collimated transmittance of rat skin tissue samples measured concurrently with administration of the 40%-glucose solution [41]. Figures 7 and 8 present the dynamics measured for skin samples with removed and not removed subcutaneous fatty layer, respectively.

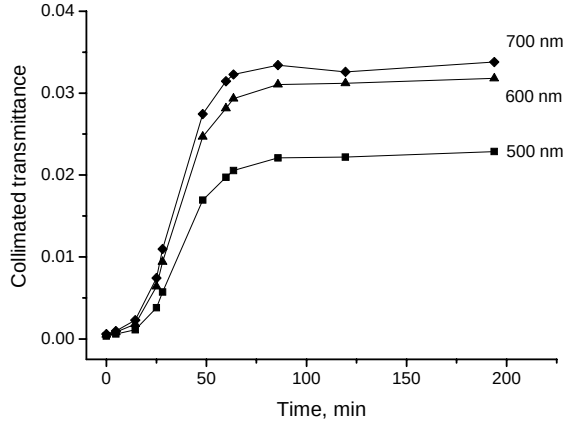

Fig. 7. The time-dependent collimated transmittance of the rat skin sample measured at different wavelengths concurrently with administration of the 40%-glucose solution [41]. Thickness of the sample is 0.57 mm.

From Fig. 7 it is seen that during first 20 minutes optical clearing of the skin samples is not observed because glucose do not penetrate into skin in this time interval. Maximal value of collimated transmittance was observed in 60 min after glucose administration, and this time is close to time of maximal optical clearing observed in case of the *in vivo* measurements (see Fig. 4).

Fig. 8 shows that penetration of glucose into the skin sample with not removed subcutaneous adipose layer have very prolonged character in contrast to data presented in Fig. 7. From Fig. 8 it is seen that during first 40 min collimated transmittance of the sample increases insignificantly and hence glucose did

not penetrate through the subcutaneous adipose layer. Glucose penetration into skin takes very long time up to four hours and the degree of the optical clearing is significantly smaller than in case of glucose penetration through skin with the removed subcutaneous adipose layer. Thus, we can conclude that in case of the *in vivo* measurements at intradermal glucose injection the glucose solution localized only within skin and not penetrate into subcutaneous muscle tissue.

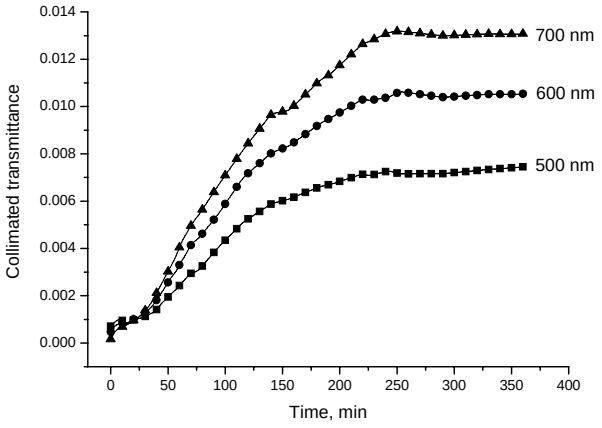

Fig. 8. The time-dependent collimated transmittance of the rat skin sample measured at different wavelengths concurrently with administration of the 40%-glucose solution [41]. Thickness of the sample is 0.73 mm.

Figure 9 presents the temporary dependencies of the blood perfusion, concentration and velocity after intradermal injection of the glucose solution. As seen from the figure the injection of glucose causes increase in the perfusion and concentration of blood, however blood velocity remains unchanged. During first ten minutes blood concentration changes insignificantly, but in the time interval from 10 to 25 minutes blood concentration increases in 5.5 folds, and then does not change.

Blood perfusion increases monotonically during first 20 minutes, and then does not change as well. At initial moment, blood velocity does not change, but in the time interval from 5 to 15 min insignificant increase of the blood velocity is observed. Later the blood velocity returns to initial value and does not change.

The result correlates well with data of the reflectance measurements, and the presented above scheme of the optical clearing. During the first 15 min after injection, glucose solution is localized in the intracutaneous vesicle. At this time the blood concentration changes insignificantly. Since 15^{th} min glucose diffuses to the tissue surrounding the vesicle and penetrates into blood vessels. Increase of glucose concentration in blood induces the increase of osmotic pressure of the blood plasma resulting in dehydration of blood erythrocytes [77] and transformation of the blood erythrocytes into echinocyte. This leads to decrease of the degree of their aggregation, hindering of formation of the coins columns, decrease of the viscosity of the blood and increase of blood flow velocity, respectively [78,79]. Thus it is explained increase of the blood flow velocity after injection. But normal tissue has sufficient regulatory ability and rheological alterations may be compensated for by an appropriate change of vascular geometry. As have been demonstrated early, increase of the osmotic pressure leads to increase in the sizes of capillaries [55] and percolation rate (the motion of the liquid of filtering in the arterial end of the capillary and reabsorbing in their venous end) [80] accordingly, i.e. to local increase of blood perfusion in the tissue.

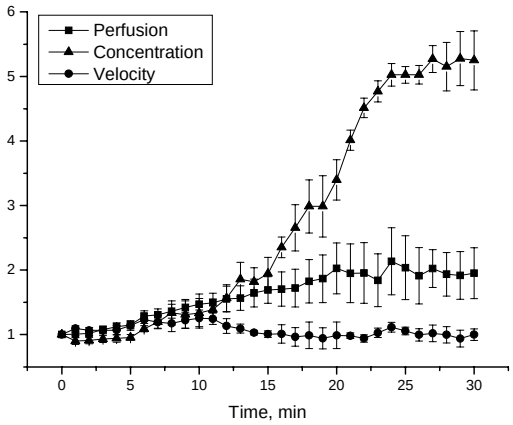

Fig. 9. The temporary dependencies of the blood perfusion (squares), concentration (circle) and velocity (up triangles) after intradermal injection of 40% glucose solution. The vertical lines show the standard deviation values.

We also assume that a considerable increase of the perfusion (about 2 folds) is caused by the amount of functioning capillaries. It is known that in the normal state the organism uses not all blood microvessels, but only part of them. For example, normal value of perfusion in skin 200 ml/100 gram min but maximum value - 497 ml/100gram min [81]. In other words, the perfusion of blood can be substantially increased due to the use of the backup capillaries. It should be noted, that the effect of increase in the number of the "open capillaries" will increase the "coefficient of diffusion" of glucose in skin and thus more rapid decrease of the skin scattering coefficient.

Acknowledgements

The research described in this publication has been made possible, in part, by grant REC-006/SA-006-00 “Nonlinear Dynamics and Biophysics” of U.S. Civilian Research and Development Foundation for the Independent States of the Former Soviet Union (CRDF) and the Russian Ministry of Science and Education; the Russian Federation President’s grant N 25.2003.2 “Supporting of Scientific Schools” and grant “Leading Research-Educational Teams” N 2.11.03 of the Russian Ministry of Science and Education.

The authors thank Dr. S.V. Eremina (Department of English and Intercultural Communication of Saratov State University) for the help in manuscript translation to English.

A.N.K. and M.S.B. gratefully acknowledge the Portuguese Ministry of Science and Technology (project SFRH/BPD/5561/2001) for financial support.

References

1. Kollias N, Stamatas G N, *Oct. JID Symposium Proc,.* 7 (2002) 64.
2. Fercher A F, Drexler W, Hitzenberger C K, Lasser T, *Rep. Prog. Phys,.* 66 (2003) 239.
3. Bigio I J, Mourant J R, *Phys. Med. Biol.,* 42 (1997) 803.
4. Thueler P, Charvet I, Bevilacqua F, Ghislain M St, Ory G, Marquet P, Meda P, Vermeulen B, Depeursinge C, *J. Biomed. Opt.,* 8 (2003) 495.
5. Andersson-Engels S, Klinteberg C, Svanberg K, Svanberg S, *Phys. Med. Biol.,* 42 (1997) 815.
6. Jacques S L, Ramella-Roman J C, Lee K, *J. Biomed. Opt.,* 7 (2002) 329.
7. Yaroslavsky A N, Neel V, Anderson R R, *J. Invest. Dermatol.,* 121 (2003) 259.
8. Liu H, Boas D A, Zhang Y, Yodh A G, Chance B, *Phys. Med. Biol.,* 40 (1995) 1983.

9. Tuchin V V *Tissue Optics: Light Scattering Methods and Instruments for Medical Diagnosis*. *Tutorial Text in Optical Engineering.* (Vol TT38 SPIE), 2000.
10. Masters B R, So P T C, *Optics Express,* 8 (2001) 2.
11. Tearney G J, Brezinski M E, Southern J F, Bouma B E, Boppart S A, Fujimoto J G, *Digestive Diseases and Sciences,* 43 (1998) 1193.
12. Tuchin V V, *J. Biomed. Opt.,* 4 (1999) 106.
13. Podoleanu A Gh, Rogers J A, Jackson D A, Dunne S, *Optics Express,* 7 (2000) 292.
14. Masters B R, So P T C, Gratton E, *Lasers Med. Sci.,* 13 (1998) 196.
15. McNichols R J, Cote G L, *J. Biomed. Opt.,* 5 (2000) 5.
16. Xu K, Li Q, Lu Z, Jiang J, *J. X-Ray Science and Technology,* 10 (2002) 187.
17. Larin K V, Motamedi M, Ashitkov T V, Esenaliev R O, *Phys. Med. Biol.,* 48 (2003) 1371.
18. de Rosa F S, Bentley M V L B, *Pharmaceutical Research,* 17 (2000) 1447.
19. Tuchin V V, Genina E A, Bashkatov A N, Simonenko G V, Odoevskaya O D, Altshuler G B, *Lasers Surg. Med.,* 33 (2003) 296.
20. Genina E A, Bashkatov A N, Simonenko G V, Odoevskaya O D, Tuchin V V, Altshuler G B, *J. Biomed. Opt.,* 9 (2004) 828.
21. Dietlein T S, Jacobi P C, Krieglstein G K, *Lasers Surg. Med.,* 23 (1998) 104.
22. Buscher B A, McMeekin T O, Goodwin D, *Lasers Surg. Med.,* 27 (2000) 171.
23. Boas D A, *Optics Express,* 1 (1997) 404.
24. Smithpeter C L, Dunn A K, Welch A J, Richards-Kortum R, *Appl. Opt.,* 37 (1998) 2749.
25. Brezinski M, Saunders K, Jesser C, Li X, Fujimoto J, *Circulation,* 103 (2001) 1999.
26. Wang R K, Xu X, Tuchin V V, Elder J B, *J. Opt. Soc. Am. B*, 18 (2001) 948.
27. Chan E K, Sorg B, Protsenko D, O'Neil M, Motamedi M, Welch A J, *IEEE J. Quantum Electronics,* 2 (1996) 943.
28. Cilesiz I F, Welch A J, *Appl. Opt.,* 32 (1993) 477.
29. Bornhop D J, Contag C H, Licha K, Murphy C J, *J. Biomed. Opt.,* 6 (2001) 106.
30. Genina E A, Bashkatov A N, Sinichkin Yu P, Kochubey V I, Lakodina N A, Altshuler G B, Tuchin V V, *J. Biomed. Opt.,* 7 (2002) 471.
31. Chance B, Liu H, Kitai T, Zhang Y, *Anal. Biochem.,* 227 (1995) 351.
32. Liu H, Beauvoit B, Kimura M, Chance B, *J. Biomed. Opt.,* 1 (1996) 200.
33. Mourant J R, Freyer J P, Hielscher A H, Eick A A, Shen D, Johnson T M, *Appl. Opt.,* 37 (1998) 3586.
34. Schmitt J M, Kumar G, *Appl. Opt.,* 37 (1998) 2788.
35. Wang R K, *J. Mod. Opt.,* 47 (2000) 103.
36. Tuchin V V, Maksimova I L, Zimnyakov D A, Kon I L, Mavlutov A H, Mishin A A, *J. Biomed. Opt.,* 2 (1997) 401.
37. Tuchin V V, Bashkatov A N, Genina E A, Sinichkin Yu P, Lakodina N A, *Tech. Physics Lett.,* 27 (2001) 489.
38. Bashkatov A N, Tuchin V V, Genina E A, Sinichkin Yu P, Lakodina N A, Kochubey V I, *Proc. SPIE,* 3591 (1999) 311.
39. Bashkatov A N, Genina E A, Kochubey V I, Lakodina N A, Tuchin V V, *Proc. SPIE,* 3908 (2000) 266.
40. Bashkatov A N, Genina E A, Korovina I V, Kochubey V I, Sinichkin Yu P, Tuchin V V, *Proc. SPIE,* 4224 (2000) 300.
41. Bashkatov A N, Genina E A, Korovina I V, Sinichkin Yu P, Novikova O V, Tuchin V V, *Proc. SPIE,* 4241 (2001) 223.
42. Bashkatov A N, Genina E A, Sinichkin Yu P, Tuchin V V, *Proc. SPIE,* 4623 (2002) 144.
43. Bashkatov A N, Genina E A, Tuchin V V, *Optical immersion as a tool for tissue scattering properties control.* (*In* Perspectives in Engineering Optics, K. Singh and V. K. Rastogi, editors. Anita Publications, New Delhi, India), 2002.
44. Bashkatov A N, Genina E A, Sinichkin Yu P, Kochubei V I, Lakodina N A, Tuchin V V, *Biophysics*, 48 (2003) 292.
45. Bashkatov A N, Genina E A, Sinichkin Yu P, Kochubey V I, Lakodina N A, Tuchin V V, *Biophys. J.,* 85 (2003) 3310.

46. Vargas G, Chan E K, Barton J K, Rylander III H G, Welch A J, *Lasers Surg. Med.,* 24 (1999) 133.
47. Vargas G, Chan K F, Thomsen S L, Welch A J, *Lasers Surg. Med.,* 29 (2001) 213.
48. Vargas G, Readinger A, Dozier S S, Welch A J, *Photochem. Photobiol.,* 77 (2003) 541.
49. Meglinskii I V, Bashkatov A N, Genina E A, Churmakov D Yu, Tuchin V V, *Quantum Electronics,* 32 (2002) 875.
50. Meglinski I V, Bashkatov A N, Genina E A, Churmakov D Y, Tuchin V V, *Laser Physics,* 13 (2003) 65.
51. Wang R K, Xu X, He Y, Elder J B, *IEEE J. Quantum Electronics,* 9 (2003) 234.
52. Wang R K, Elder J B, *Lasers Surg. Med.,* 30 (2002) 201.
53. Wang R K, Tuchin V V, *J. X-Ray Science and Technology,* 10 (2002) 167.
54. Viator J A, Choi B, Peavy G M, Kimel S, Nelson J S, *Phys. Med. Biol.,* 48 (2003) N15.
55. Galanzha E I, Tuchin V V, Solovieva A V, Stepanova T V, Luo Q, Cheng H, *Appl. Phys. D,* 36 (2003) 1739.
56. Xu X, Wang R, Elder J B, *Appl. Phys. D,* 36 (2003) 1707.
57. Genina E A, Bashkatov A N, Kochubey V I, Tuchin V V, *Optics and Spectroscopy,* 98 (2005) 470.
58. Tuchin V V, Xu X, Wang R K, *Appl. Opt.,* 41 (2002) 258.
59. Xu X, Wang R K, Elder J B, Tuchin V V, *Phys. Med. Biol.,* 48 (2003) 1205.
60. Tuchin V V, Zhestkov D M, Bashkatov A N, Genina E A, *Optics Express,* 12 (2004) 2966.
61. Schaefer H, Redelmeier T E, *Skin Barrier*. (Karger), 1996.
62. Corcuff P, Fiat F, Minondo A-M, *Skin Pharmacology and Applied Skin Physiology,* 14 (2001) 4.
63. Blank I H, Moloney J, Emslie A G, Simon I, Apt C, *J. Invest. Dermatol.,* 82 (1984) 188.
64. Guy R H, Delgado-Charro M B, Kalia Y N, *Skin Pharmacology and Applied Skin Physiology,* 14 (2001) 35.
65. Aspress N, Egerton I B, Lim A C, Shumack S P, *Austral. J. Dermatol.,* 44 (2003) 19.
66. Stenn K S, *The skin.* (*In* Cell and Tissue Biology, ed by L Weiss, Urban & Shwarzenberg, Baltimore), 1988.
67. Odland G F, *Structure of the skin* (*In* Physiology, Biochemistry, and Molecular Biology of the Skin, vol. 1, ed by L A Goldsmith, Oxford University Press, Oxford), 1991.
68. Ryan T J, *Cutaneous Circulation* (*In* Physiology, Biochemistry, and Molecular Biology of the Skin, vol. 1, ed by L A Goldsmith, Oxford University Press, Oxford), 1991.
69. Chedekel M R, *Photophysics and photochemistry of melanin* (*In* Melanin: Its Role in Human Photoprotection, eds. L Zeise, M R Chedekel and T B Fitzpatrick Overland Park, Valdenmar), 1995.
70. Taton' Y, *Obesity. Pathphysiology, Diagnostics, Therapy.* (Medical Press, Warsaw), 1981.
71. Shurigin D Ya, Vyazitskiy P O, Sidorov K A, *Obesity.* (Medicine, Leningrad), 1975.
72. Gurr M I, Jung R T, Robinson M P, James W P T, *Int. J. Obesity,* 6 (1982) 419.
73. Smith R C, Baker K S, *Appl. Opt.,* 20 (1981) 177.
74. Galanzha E.I., Tuchin V.V., Luo Q., Cheng H., Solov'eva A.V., *Asian J. Physics*, 10 (2001) 503.
75. Collins R. E., *Flow of fluids through porous materials.* (Reinhold Publishing Corporation, New York), 1961.
76. Isichenko M B, *Rev. Mod. Phys.,* 64 (1992) 961.
77. Bashkatov A N, Zhestkov D M, Genina E A, Tuchin V V, *Optics and Spectroscopy,* 98 (2005) 695.
78. *Human Physiology.* (Edited by R.F. Smidth and G. Thews, Springer-Verlag, Berlin, Heidelberg, New York, London, Paris, Tokio, HongKong), 1989.
79. Popel A S, Pittman R N, *Mechanics and transport in the microcirculation.* (*In* The biomedical engineering handbook, Editor-in-chief Joseph D. Bronsino, CRC Press), 1995.
80. Koscielny J, Latza R, Wolf S, Kiesewetter H, Jung F, *Clinical Hemorheology and Microcirculation,* 19 (1998) 139.
81. Davidson J A, Gir S, Paul J, *J. Biomed. Mat. Res.*, 22 (1988) 281.

[*Received*: 1.11.2005]